

Earth's Future

RESEARCH ARTICLE

10.1029/2022EF002900

Key Points:

- We develop a photosynthesis and transpiration model to account for different light spectra
- The red part of the light spectrum is more efficient for plant photosynthesis and water use
- The blue part of the light spectrum could be used for solar energy production

Supporting Information:

Supporting Information may be found in the online version of this article.

Correspondence to:

M. Abou Najm,
mabounajm@ucdavis.edu

Citation:

Camporese, M., & Abou Najm, M. (2022). Not all light spectra were created equal: Can we harvest light for optimum food-energy co-generation? *Earth's Future*, 10, e2022EF002900. <https://doi.org/10.1029/2022EF002900>

Received 10 MAY 2022



Accepted 10 NOV 2022

Author Contributions:

Conceptualization: Majdi Abou Najm
Data curation: Matteo Camporese
Formal analysis: Matteo Camporese
Investigation: Matteo Camporese, Majdi Abou Najm
Methodology: Matteo Camporese, Majdi Abou Najm
Software: Matteo Camporese
Validation: Matteo Camporese, Majdi Abou Najm
Visualization: Majdi Abou Najm
Writing – original draft: Matteo Camporese
Writing – review & editing: Majdi Abou Najm

© 2022 The Authors. *Earth's Future* published by Wiley Periodicals LLC on behalf of American Geophysical Union. This is an open access article under the terms of the [Creative Commons Attribution License](https://creativecommons.org/licenses/by/4.0/), which permits use, distribution and reproduction in any medium, provided the original work is properly cited.

Not All Light Spectra Were Created Equal: Can We Harvest Light for Optimum Food-Energy Co-Generation?

Matteo Camporese¹  and Majdi Abou Najm^{2,3} 

¹Department of Civil, Environmental and Architectural Engineering, University of Padova, Padova, Italy, ²Department of Land, Air and Water Resources, University of California, Davis, Davis, CA, USA, ³UC Davis Institute of the Environment, University of California, Davis, Davis, CA, USA

Abstract Humanity's growing appetites for food and energy are placing unprecedented yield targets on our lands. Chasing those ever-expanding land intensification targets gave rise to monocultures and sharpened the divide between food and energy production groups. Here, we argue that this does not have to be a zero-sum game if food and energy can be co-generated in the same land. Co-generation can lead to sustainable intensification but requires a paradigm shift in the way we manage our resources, particularly light. Using an extended model of plant photosynthesis and transpiration, we demonstrate how plants react to different incident light spectra and show that manipulating light could be effective for boosting land and water efficiencies, thus potentially improving soil health. This knowledge can possibly unlock the real potential of promising modern agricultural technologies that target optimization of light allocations such as agrivoltaics. This study suggests that the blue part of the light spectrum is less efficient in terms of carbon assimilation and water use and could be more effectively used to produce solar energy, while the red part could efficiently produce biomass. A sensitivity analysis to the most important crop and environmental variables (irradiance, air temperature, humidity, and CO₂ concentration) shows that plant response to different light treatments is sensitive to environmental boundary conditions and is species-specific. Therefore, further research is necessary to assess which crops and climates are more suitable to optimize the proposed food-water-energy nexus.

Plain Language Summary Achieving sustainability for the deeply interlinked water, energy, and food systems requires revolutionary, rather than incremental, solutions at their nexus. This includes forms of food and energy co-generation like agrivoltaics, which can boost land and water efficiencies and improve soil health. Advancements along those lines require deep understanding of how plants react to different incident light spectra. In this paper, we demonstrate the importance of different light spectra, and show that those spectra, if optimized in terms of their utilization, could lead to sustainable and more efficient food and energy systems. For example, the red part of the light spectrum is more efficient in terms of carbon assimilation and water use while the blue part could be more effectively used to produce solar energy.

1. Introduction

Projections show that by 2050, we will need 60% more food and 40% more water to satisfy the demands of our growing population, all this in addition to 50% more energy thus adding significant stress at the nexus between water, energy, and food (Ringler et al., 2016). These sustainability challenges are, unfortunately, highly interconnected (Chamas et al., 2021; Higgins & Najm, 2020). We say unfortunately because solving those challenges one problem at a time often ends up creating many more. Revolutionary solutions are needed along the water, energy and food nexus for addressing those grand challenges, and one possible game-changer is a resource that is often taken for granted and treated as a boundary condition in agriculture and energy generation. This resource is light, currently an external forcing dictating water budgets for agricultural fields and imposing upper limits of kilowatt-hour production in solar farms. Here, we present light differently (Figure 1a): a multi-spectral resource that can be allocated based on need, thus allowing for dual or multiple uses at the same location. Considering light from that perspective can significantly contribute to the advancement of an entire suite of agricultural innovations, from agrivoltaics (Abidin et al., 2021; Barron-Gafford et al., 2019) to hydroponics (Ragaveena et al., 2021), all spurred by recent advances in photovoltaic (PV) and light-emitting diode (LED) technologies (Emmott et al., 2015; Pattison et al., 2018; Pinho et al., 2012; Waller et al., 2021).

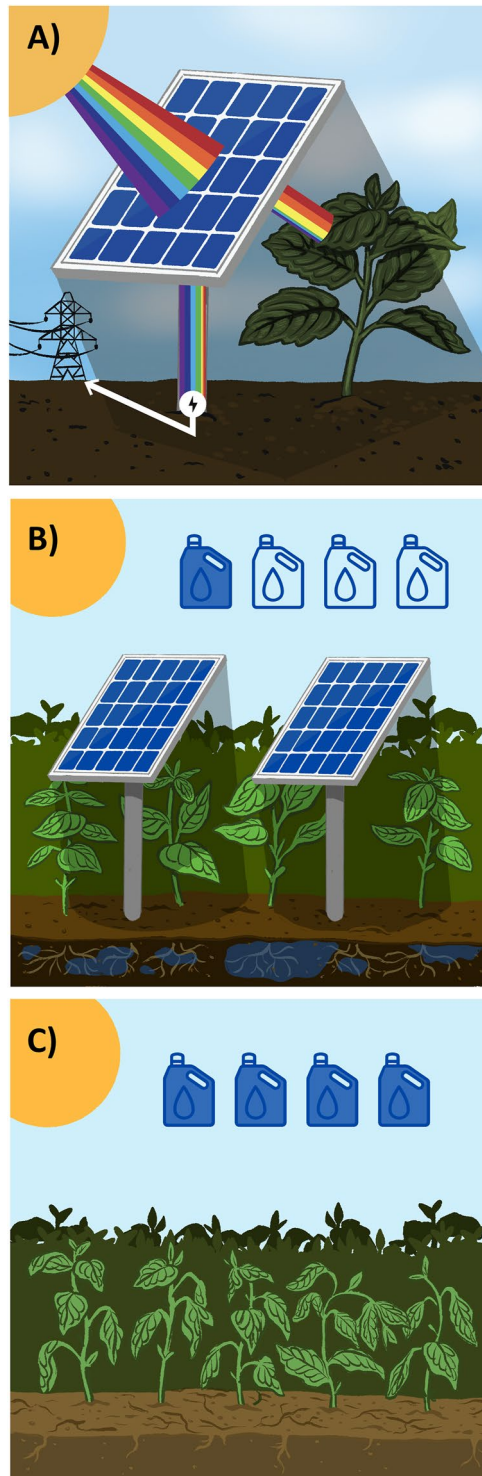


Figure 1. (a) Schematization of the light treatment concepts demonstrating how incoming solar radiation with full spectrum ranging from blue to red can be divided into energy-generating blue-centered spectra and plant-efficient red-centered spectra. (b) A schematic of an agrivoltaic concept where the shade produced by photovoltaic panels can reduce crop yields of some crops, but such losses can be offset by the energy produced leading to overall efficiencies (Land Equivalent Ratios) that exceed 100%, in addition to water saved and longer soil moisture retention. (c) A schematic of a classic farm with potentially higher crop yields for sun-loving plants, but at an overall less efficient land equivalent ratio and possibly higher water requirements.

Furthermore, this does not end with indoor farming and energy-intensive food production facilities. Outdoor agrivoltaics is a promising technology that can provide more food and energy with less water and land, thus maximizing the land and water efficiencies and leading to a healthier nexus (Barron-Gafford et al., 2019; Fernández et al., 2022; Feuerbacher et al., 2021). The recent development of semi-transparent photo-selective organic PV arrays (Magadley et al., 2022; Waller et al., 2021) potentially allows for the optimization and control of lighting treatments and the simultaneous allocation of light for multiple uses like food and energy co-generation (Emmott et al., 2015; Magadley et al., 2022). This is however crop and climate dependent, and achieving the real potential of agrivoltaics requires a deeper understanding of plants response to different light spectra, thus allowing optimization of the solar spectrum between food and energy production in the same land. This can lead to more water-efficient production of food, longer moisture retention, and the co-generation of kilowatt-hours of electricity from excess light spectra that would have increased crop water demands (Figures 1b and 1c).

Within this context, advancing knowledge in plant response to different light spectra (Smith et al., 2017) is a key and necessary (although not sufficient) step to design systems capable of achieving sustainable land management with optimum crop productivity and water use. This requires simultaneous developments in lab, greenhouse and field experiments along with calibrated and validated numerical models. It has long been known that some plants and crops may benefit from partial shading (Inada & Nishiyama, 1987), which implies not only reduced light intensity, but also modified spectral quality due to selected attenuation of radiation by the canopy. More recently, many experimental studies have been conducted to investigate how crops (especially herbal crops such as lettuce, basil, soybean, etc.) react to different light treatments in laboratory controlled conditions (Ahmed et al., 2020; Chen et al., 2021; Clavijo-Herrera et al., 2018; Danziger & Bernstein, 2021; Fang et al., 2021; Kang et al., 2021; Kim et al., 2004; Lim & Kim, 2021; Liu et al., 2017; Mochizuki et al., 2019; Muneer et al., 2014; Nguyen & Oh, 2021; Pennisi et al., 2019; Pennisi, Pistillo, Orsini, Cellini, et al., 2020; Pennisi, Pistillo, Orsini, Gianquinto, et al., 2020; Pundir et al., 2020; Samuolienė et al., 2020). The majority of these studies, although sometimes with contrasting results, suggest that some parts of the light spectrum are less efficient in terms of carbon assimilation and water use and could be more effectively used to produce solar energy. Studies under field conditions where photo-selective shade nets were applied to lettuce (Amaro de Sales et al., 2021), apple trees (Bastías et al., 2021), and grapevine (Marigliano et al., 2022; Martínez-Lüscher et al., 2017) also suggest that proper sunlight management can lead to improved crop performance, higher water use efficiency (WUE), and mitigation of heat wave damage.

In spite of the recent abundance of experimental results, no model so far has been developed that can explicitly account for the effect of different light spectra on plant gas exchanges, which exert a fundamental control on productivity and yield. Including the effects of spectral quality in crop modeling is therefore more important than ever, given the increasing interest in simulating water management and crop productivity in agrivoltaic systems (Elamri et al., 2018). Achieving this requires, as a first step, to compute photosynthesis and transpiration rates as a function of incident light spectral quality.

Here, we present an expanded model of coupled photosynthesis and transpiration based on the full spectra of incident light and plant response functions, namely absorptance and quantum yield. The model capabilities are assessed by testing its ability to correctly simulate the reported response of different plant types to various light treatments. The main goal of this study is to illustrate how some lighting conditions can result in improved productivity, in terms of net CO₂ assimilation rate, and reduced water use for two representative plant types and to discuss potential implications and relevant applications for modern technologies that could lead to more sustainable food and energy co-generation.

2. Materials and Methods

Building upon Daly et al. (2004) and Fatichi et al. (2012), we developed and tested an extended model of plant photosynthesis and transpiration that is able to reproduce the response of various C3 plant types treated with different light spectra. The model is based on the full spectra of incident light and plant response functions, namely absorptance and quantum yield. The model capabilities were assessed by testing its ability to correctly simulate the reported response of different plant types to various light treatments. The model includes the following modules for the computation of stomatal conductance, photosynthesis rate, and transpiration, based on the full spectra of incident light and photosynthetically active radiation (PAR) curves. Figure 2 reports the flowchart of the model.

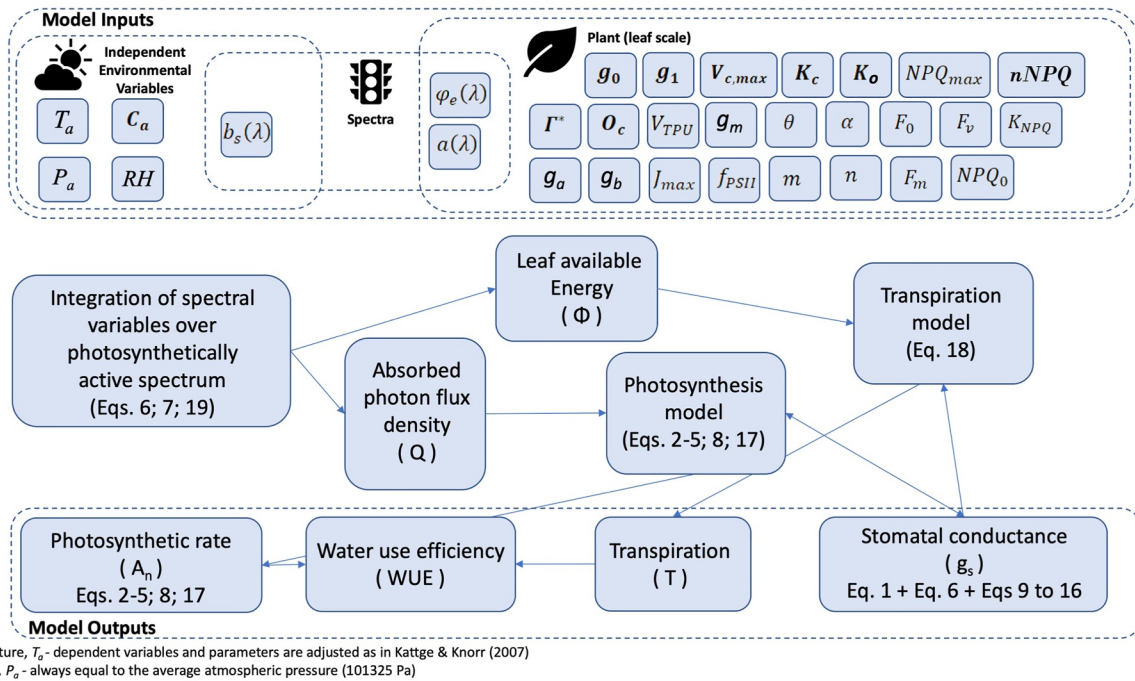


Figure 2. Flowchart of the proposed model of coupled photosynthesis and transpiration, indicating input variables, simulated processes, and outputs.

2.1. Stomatal Conductance Model

Plants control the opening of the stomata to regulate the transfer of water and CO_2 during transpiration and photosynthesis. The complex mechanisms of stomatal movement depend on both plant physiology and environmental factors. Although no complete model for their functioning has been developed so far, a wide variety of models for stomatal conductance exist, ranging from very detailed to more simplified descriptions (Buckley, 2017). Here, we used the model proposed by Medlyn et al. (2011) as modified by Kromdijk et al. (2019) to explicitly consider light-induced stomatal movements:

$$g_s = g_0 + 1.64 \times \left(1 + \frac{g_1}{\sqrt{VPD_A}} \right) \times \frac{1 - q_L}{C_a}, \quad (1)$$

where g_s is stomatal conductance in $mol\ H_2O\ m^{-2}\ s^{-1}$, g_0 and g_1 are an intercept and slope parameters, respectively, VPD_A is the atmospheric water vapor pressure deficit, computed from the air relative humidity (RH), C_a is the CO_2 concentration surrounding the leaf, and $1 - q_L$ is the fluorescence parameter estimating the light-induced changes in the redox state of quinone A, which have been shown to be strongly linked to stomatal conductance in tobacco (Głowacka et al., 2018).

2.2. The Farquhar-Von Caemmerer-Berry (FvCB) Photosynthesis Model

Stomatal conductance needs to be incorporated into a photosynthesis model. The widely used biochemical model of leaf photosynthesis by Farquhar et al. (1980), hereafter Farquhar-Von Caemmerer-Berry (FvCB), is used here in conjunction with the stomatal model of Equation 1. The FvCB model computes the net CO_2 assimilation rate (A_n) as the minimum of three limiting factors: the Rubisco-limited rate (A_c), the RuBP regeneration-limited (light-limited) rate (A_j), and the triose phosphate utilization limited rate (A_{TPU}):

$$A_c = \frac{V_{c,max} \times (C_c - \Gamma^*)}{C_c + K_c \times \left(1 + \frac{O_c}{K_o} \right)} - R_d, \quad (2)$$

$$A_j = \frac{J \times (C_c - \Gamma^*)}{4C_c + 8\Gamma^*} - R_d, \quad (3)$$

$$A_{\text{TPU}} = 3V_{\text{TPU}} - R_d, \quad (4)$$

$$A_n = \min(A_c, A_J, A_{\text{TPU}}), \quad (5)$$

where $V_{c,\text{max}}$ is the maximum rate of RuBP carboxylation, K_c and K_o are the Michaelis-Menten constants to describe CO_2 and O_2 effects on RuBP carboxylation, C_c is the CO_2 concentration in the leaf pores, Γ^* is the CO_2 compensation point in the absence of R_d , which represents mitochondrial respiration not associated with photorespiration, J is the rate of whole-chain electron transport, V_{TPU} is the maximum rate of triose phosphate utilization, and O_c is the O_2 concentration in the chloroplast, which we assume equal to ambient concentration. Temperature dependence in the model is taken into account as in Kattge and Knorr (2007), while the CO_2 compensation point is calculated as in Leuning (1995).

2.3. Extension of the FvCB Model to Consider Light Spectra

The actual rate of whole-chain electron transport, J in Equation 3, is modeled as a function of the incident photon irradiance spectrum, $b_s(\lambda)$, the plant absorptance spectrum, $a(\lambda)$, and the relative quantum yield spectrum, $\varphi_e(\lambda)$ (i.e., the quantum yield spectrum normalized with respect to its maximum value, α) all of them expressed as functions of the wavelength, λ . The absorbed photon irradiance, PFD_{abs} , can be expressed as the integration over the visible spectrum of the incident photon irradiance weighed through the plant absorptance:

$$\text{PFD}_{\text{abs}} = \int b_s(\lambda)a(\lambda)d\lambda, \quad (6)$$

while the corresponding potential rate of electron transport, Q , is:

$$Q = \alpha \int b_s(\lambda)a(\lambda)\varphi_e(\lambda)d\lambda, \quad (7)$$

Next, J can be calculated using the well-known expression for the non-rectangular hyperbola:

$$J = \frac{Q \times f_{\text{PSII}} + J_{\text{max}} - \sqrt{(Q + J_{\text{max}})^2 - 4 \times \theta \times Q \times f_{\text{PSII}} \times J_{\text{max}}}}{2 \times \theta}, \quad (8)$$

where f_{PSII} represents the proportion of absorbed light partitioned to photosystem II, J_{max} is the maximum rate of whole-chain electron transport and θ is a shape factor (Ogren & Evans, 1993). Photosystem II is the first protein complex in the light-dependent reactions of oxygenic photosynthesis and provides the electrons for all of photosynthesis to occur.

2.4. Light-Induced Changes in Stomatal Conductance

In order to compute the stomatal conductance with Equation 1, we must evaluate q_L . To do so, we follow the method proposed in Kromdijk et al. (2019). We start by calculating the operating efficiency of photosystem II, Φ_{PSII} , as:

$$\Phi_{\text{PSII}} = \frac{J}{\text{PFD}_{\text{abs}} \times f_{\text{PSII}}}. \quad (9)$$

Then, a sigmoidal Hill function is used to describe the steady-state level of non-photochemical quenching (NPQ) as a function of PFD_{abs} :

$$\begin{cases} \text{NPQ} = \text{NPQ}_0 + \frac{\text{NPQ}_{\text{max}} - \text{NPQ}_0}{\left[\left(\frac{K_{\text{NPQ}}}{\text{PFD}_{\text{abs}}} \right)^{n_{\text{NPQ}}} + 1 \right]} & \text{if } \text{PFD}_{\text{abs}} > 0 \\ \text{NPQ} = 0 & \text{if } \text{PFD}_{\text{abs}} = 0 \end{cases}, \quad (10)$$

where NPQ_0 is the basal level of NPQ, K_{NPQ} is photon irradiance at half amplitude, and n_{NPQ} and NPQ_{max} are the Hill coefficient and asymptote, respectively. NPQ is a mechanism employed by plants to protect themselves

from the adverse effects of high light intensity, whereby excess excitation energy is dissipated as heat, helping to regulate and protect photosynthesis in environments where light energy absorption exceeds the capacity for light utilization.

The maximal fluorescence without dark-adaptation at a given light level (F'_m) is calculated from NPQ and dark-adapted maximal fluorescence (F_m) according to:

$$F'_m = \frac{F_m}{\text{NPQ} + 1}. \quad (11)$$

The corresponding level of F' is computed as:

$$F' = F'_m \times (1 - \Phi_{\text{PSII}}). \quad (12)$$

Next, the minimal fluorescence without dark-adaption (F'_0) is evaluated by first considering the effects of fluorescence suppression via NPQ:

$$F'_{\text{0NPQ}} = \frac{F_0}{\frac{F_v}{F_m} + \frac{F_0}{F'_m}}, \quad (13)$$

$$\left(\frac{F'_v}{F'_m}\right)_{\text{NPQ}} = 1 - \frac{F'_{\text{0NPQ}}}{F'_m}, \quad (14)$$

and then by using an empirical relationship to predict the elevation of fluorescence due to inactivation of reaction centers:

$$1 - \frac{\left(\frac{F'_v}{F'_m}\right)}{\left(\frac{F'_v}{F'_m}\right)_{\text{NPQ}}} = m \times \left(0.5 \times \text{PFD}_{\text{abs}} \times \frac{F'}{F'_m}\right) + n \quad (15)$$

where $F_v = F_m - F_0$, $F'_v = F'_m - F'_0$, and m and n are empirical coefficients that must be fitted on light response curves of chlorophyll parameters.

Combining Equation 15 with Equations 11 and 12 yields q_L as:

$$q_L = \frac{F'_m - F'}{F'_m - F'_0} \times \frac{F'_0}{F'}. \quad (16)$$

Note that q_L does not depend on the single values of F_m and F_0 , but on the ratio F_v/F_0 , which is typically in the range 0.6–0.8.

2.5. Coupling Stomatal Conductance and Photosynthesis Models

Once the stomatal conductance is computed, as C_c is not known a priori, A_n can be calculated by solving iteratively for Equations 2–4 and:

$$C_c = C_a - A_n \left(\frac{1.64}{g_s} + \frac{1}{g_m} + \frac{1.37}{g_b} + \frac{1}{g_a} \right), \quad (17)$$

where g_m , g_b , and g_a are mesophyll, leaf boundary layer, and atmospheric boundary layer conductances, respectively.

2.6. Transpiration Model

The stomatal conductance is also needed to compute transpiration, T , which is the driver of root water uptake, that is, the water used by a plant. Under the assumption of steady state, water storage changes in the plant are neglected and root water uptake is equal to transpiration. This can be modeled through the Penman-Monteith approach, as in Daly et al. (2004).

$$T = \frac{(\lambda_w \gamma_w g_{ba} \rho D + S \Phi) g_s}{\rho_w \lambda_w [\gamma_w (g_{ba} + g_s) + g_s S]}, \quad (18)$$

where λ_w is the latent heat of water vapourization, $\gamma_w = p_a c_p / (0.622 \lambda_w)$ is the psychrometric constant, with p_a being atmospheric pressure and c_p the specific heat of air, D is the difference between specific humidity at saturation and at air temperature T_a , S is the slope of the curve relating saturation vapor pressure to temperature, Φ is the leaf available energy, and $g_{ba} = (g_a^{-1} + g_b^{-1})^{-1}$ is the series conductance of the leaf boundary layer and atmospheric boundary layer. Note that in Equation 18 transpiration refers to the water flux for unit leaf surface, not the entire canopy.

The leaf available energy in Equation 18 is calculated from the photon irradiance spectrum and the plant absorbance function as:

$$\Phi = \int b_s(\lambda) a(\lambda) \frac{hc}{\lambda} N_A d\lambda, \quad (19)$$

where h is the Planck constant, c is the speed of light, and N_A is the Avogadro number.

Under the simplifying assumption that CO_2 assimilation rate is well correlated to crop yield, the WUE here is calculated as $\text{WUE} = 44 \times A_n / (18 \times T)$, expressed in mass of CO_2 assimilated per mass of water used.

2.7. Model Assessment

To assess the capabilities of the model to reproduce the plant response to different light treatments, we simulated photosynthesis and transpiration with the conditions of four studies carried out in controlled laboratory experiments. In these four studies (Clavijo-Herrera et al., 2018; Lim & Kim, 2021; Mochizuki et al., 2019; Pennisi et al., 2019), various crops (lettuce, basil, and strawberry) were subjected to different light treatments (Figure S1 in Supporting Information S1) based on several combinations of LED lights and other artificial lighting systems. The stomatal conductance was measured in all these experiments, while water use and photosynthetic rate were either measured or assessed with different approaches, as reported in Table S1 in Supporting Information S1.

As the model outputs depend on many parameters, some of them plant-specific, model calibration was necessary to ensure that simulations reproduced the observed variables satisfactorily. To this end, the most sensitive parameters, namely $V_{c,\max}$, J_{\max} , g_0 , g_1 , θ , and α , were tuned using the Shuffled Complex Evolution method (Duan et al., 1994). Further details are reported in Table S2 in Supporting Information S1. Furthermore, to take into account the limited knowledge of ventilation conditions in the experiments, relevant for the computation of transpiration, the leaf and atmospheric boundary layer conductances were also calibrated, always assuming that $g_b = g_a$. All other parameters were taken as in Kromdijk et al. (2019).

Figure S3 in Supporting Information S1 shows the model capabilities to reproduce photosynthetic rate, A_n , stomatal conductance, g_s , and water use (either in terms of transpiration, T , or water use efficiency, $\text{WUE} = A_n / T$) in three different experimental studies, where lettuce (Clavijo-Herrera et al., 2018) and basil (Lim & Kim, 2021; Pennisi et al., 2019) were subjected to different light treatments (Figure S1 in Supporting Information S1). The color of the data points indicates the dominant part of the spectrum in the different treatments. Overall, the model simulates the observations quite satisfactorily, with a generally significant correlation between computed and observed variables. The match is particularly good for stomatal conductance in all the three test cases (Figures S3b, S3e, and S3h in Supporting Information S1), highlighting that g_s generally increases with the percentage of blue light. However, while this increase typically translates into higher transpiration (Figures S3i in Supporting Information S1), it does not necessarily imply a higher CO_2 assimilation rate (Figures S3a, S3d, and S3g in Supporting Information S1), generally resulting in a decreased WUE (Figures S3c and S3f in Supporting Information S1).

The model has also been tested against data taken from Mochizuki et al. (2019), who measured the response of strawberry plants to increasing photon flux density, under three different light treatments, namely blue, green, and red LEDs. As a member of the Rosaceae family, strawberry is characterized by absorbance and quantum yield spectra more similar to other fruit trees of the same family (e.g., peach and almond) than those used previously for lettuce and basil (Inada, 1976), which are more typical of herbaceous crops. Model results are presented in

Figure S4 in Supporting Information S1, in comparison with observed photosynthetic rate, stomatal conductance, transpiration, and intercellular CO₂ concentration. As for lettuce and basil, simulations and observations agree that, also for strawberry plants, the stomatal conductance (Figure S4c in Supporting Information S1) is highest under the blue light treatment, followed by the green light and the red light. The same mutual relations hold for transpiration (Figure S4b in Supporting Information S1) and intercellular CO₂ concentration (Figure S4d in Supporting Information S1), while the differences in photosynthetic rates (Figure S4a in Supporting Information S1) are not as significant, in agreement with Mochizuki et al. (2019), especially between the red and green lighting treatments. This again leads to the blue LED treatment being less efficient from a water use perspective.

Overall, the comparison between experimental data and model simulations shown in Figures S3 and S4 in Supporting Information S1 is satisfactory and provide us with enough confidence that the model is able to reliably reproduce the gas exchange fluxes between plants and atmosphere under different light treatments.

3. Results

To gain relevant insights on the possible implications of different light treatments on crop production and water use, we carried out a sensitivity analysis on the model by running a number of simulations changing one environmental input at a time and leaving the others fixed with respect to a reference simulation. The response of photosynthetic rate (A_n), transpiration (T), stomatal conductance (g_s), WUE, and intercellular-atmospheric CO₂ concentration ratio (C_i/C_a) were modeled as a function of changing irradiance ($W\ m^{-2}$), temperature ($^{\circ}C$), vapor pressure deficit (KPa), and atmospheric CO₂ concentration (ppm), with incident light spectra as reported in Figure S5 in Supporting Information S1.

The plant sensitivity to light spectral quality was analyzed using, as references, the calibrated parameter data sets for basil and strawberry from Pennisi et al. (2019) and Mochizuki et al. (2019), respectively (see Figure S2 and Table S2 in Supporting Information S1, for more details), and using environmental variables representative of growth chambers (for basil) and agrivoltaic fields (for strawberry). In the first case, reference values for irradiance, temperature, RH, and air CO₂ concentration were 80 $W\ m^{-2}$, 24 $^{\circ}C$, 70%, and 450 ppm, respectively. In the second case, we used values typical of the central California average climate in the growth season, that is, 25 $^{\circ}C$, 41.2%, and 410 ppm, for temperature, RH, and air CO₂ concentration, respectively, while keeping irradiance at 80 $W\ m^{-2}$.

Figure 3 reports the results of the sensitivity analysis with basil parameters, with line colors indicating the dominant part of the spectrum (between red and blue, plus green for a broad-spectrum artificial light) and black denoting the reference solar light spectrum (Gueymard et al., 2002). The first column of panels shows the sensitivity of the variables to irradiance ($W\ m^{-2}$) with blue-dominated light treatments resulting in increased stomatal conductance (Figure 3c) and transpiration (Figure 3b), although not associated to an increase in photosynthetic rates (Figure 3a). This suggests that in a blue to red comparison the red spectrum is consistently more efficient for plant growth, as demonstrated by higher WUE (Figure 3d) compared to blue. This is further confirmed by the inspection of the C_i/C_a ratio (Figure 3e), which shows consistently larger values with increasing blue light fractions, until irradiances of about 300 $W\ m^{-2}$, after which the light saturation effect comes into play and all curves tend to collapse on each other. Interestingly, the solar light and broad-spectrum LED light (the artificial lighting with a spectrum more similar to the solar spectrum) exhibits reduced transpiration compared to all blue-red light combinations, resulting in larger WUE values starting from around 150 $W\ m^{-2}$. The second panel column reports the sensitivity to air temperature ($^{\circ}C$), whereby photosynthetic rate (Figure 3f) exhibits the typical bell-shaped curve with a maximum around 15 $^{\circ}C$ –18 $^{\circ}C$ depending on the light treatment, whereas transpiration (Figure 3g) follows an overall monotonic increasing trend, with a notable exception for the two “reddest” treatments, due to a minimum of stomatal conductance around 30 $^{\circ}C$ (Figure 3h). As a result, the WUE also displays a maximum value for all the light treatments, varying from about 10 $^{\circ}C$ –15 $^{\circ}C$. Once more, increasing the fraction of blue light results in less CO₂ assimilation and more water consumption. This holds true also when changing vapor pressure deficit (third column, Figures 3k–3o) and air CO₂ concentration (fourth column, Figures 3p–3t). Comparing Figure 3p with Figure 3a, it is apparent that increasing CO₂ concentration enhances the differences between different light treatments, as opposed to increasing irradiance. This could have important implications for the potential use of LED technologies for artificial and/or supplemental lighting of crops in the context of climate change and predicted increase of c_a .

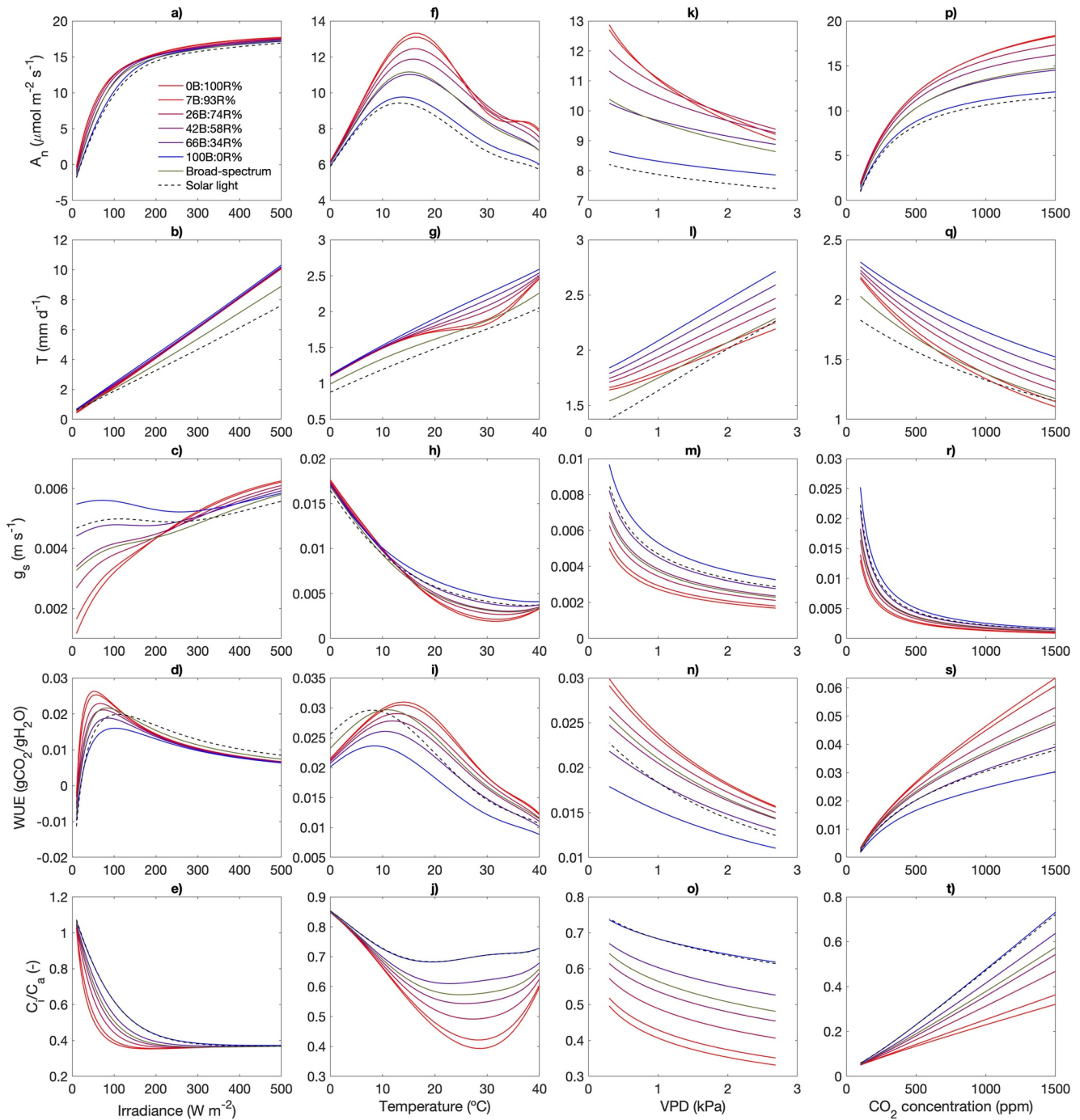


Figure 3. (a, f, k, and p) Photosynthesis rate, (b, g, l, and q) transpiration, (c, h, m, and r) stomatal conductance, (d, i, n, and s) water use efficiency, and (e, j, o, and t) intercellular/atmospheric CO_2 concentration ratio as a function of (a–e) irradiance, (f–j) air temperature, (k–o) vapor pressure deficit, and (p–t) atmospheric CO_2 concentration for basil subject to various light treatments. The reference values for the environmental variables are representative of common conditions in growth chambers, that is, 80 W m^{-2} , 24°C , 70%, and 450 ppm for irradiance, temperature, relative humidity, and air CO_2 concentration, respectively.

Figure 4 reports analogous results for the strawberry-optimized set of parameters. Overall, the differences between the various light treatments are less pronounced compared to the basil-optimized parameters (Figure 4) but generally follow similar trends. Furthermore, the optimum range of temperatures for photosynthetic rate and WUE is generally shifted toward higher temperatures. For this type of plant, the blue light seems even less favorable, with values of A_n smaller than the ones resulting from the application of the solar light spectrum (e.g.,

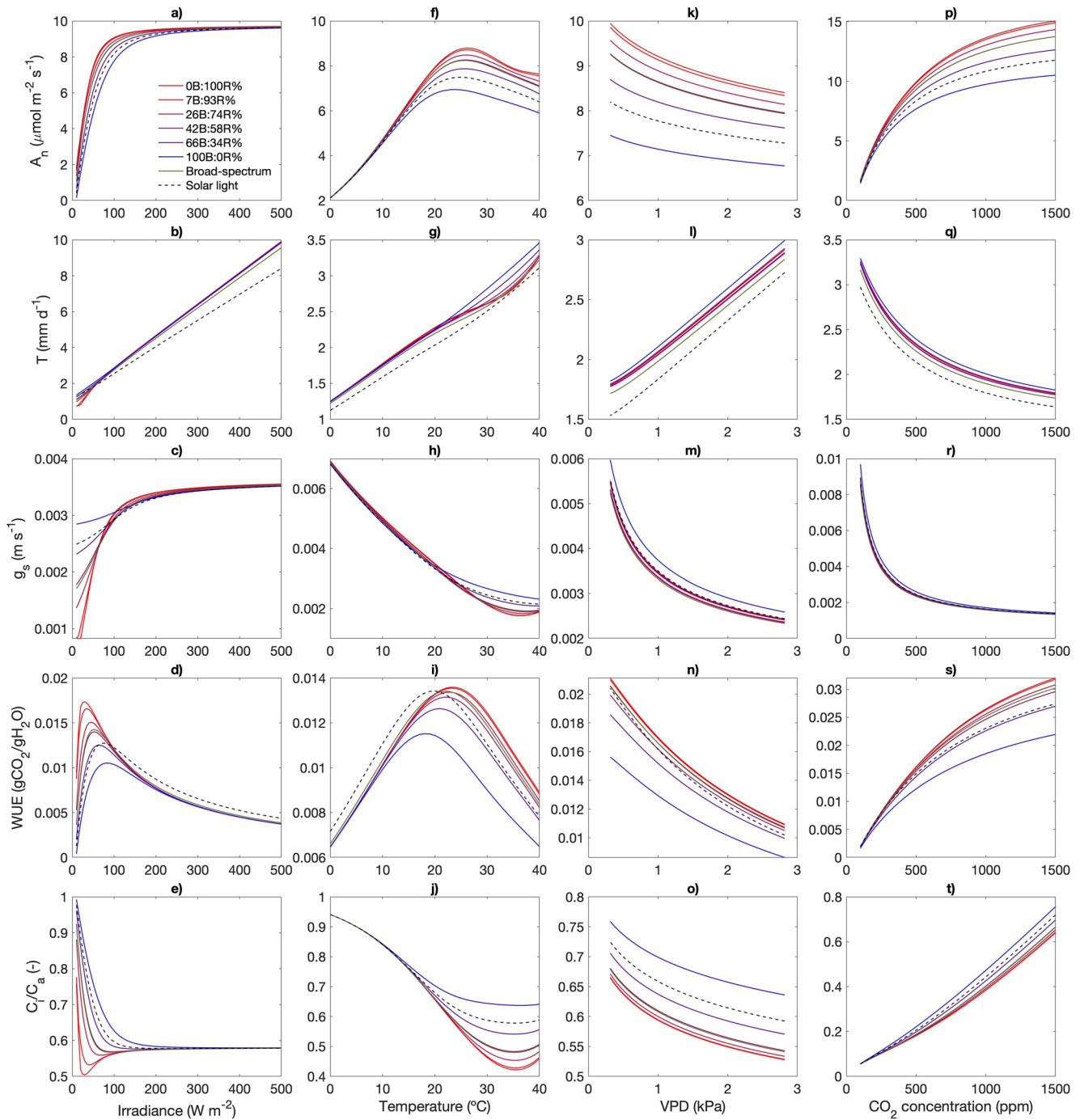


Figure 4. (a, f, k, and p) Photosynthesis rate, (b, g, l, and q) transpiration, (c, h, m, and r) stomatal conductance, (d, i, n, and s) water use efficiency, and (e, j, o, and t) intercellular/atmospheric CO_2 concentration ratio as a function of (a–e) irradiance, (f–j) air temperature, (k–o) vapor pressure deficit, and (p–t) atmospheric CO_2 concentration for strawberry subject to various light treatments. Except for irradiance (80 W/m^2 , as for basil), the reference values for temperature, relative humidity, and air CO_2 concentration are representative of the central California average climate in the growth season, that is, 25°C , 41.2% , and 410 ppm , respectively.

compare Figures 4f and 4p with Figures 3f and 3p). Overall, the model suggests that plants with absorptance and quantum yield similar to strawberry are less productive, showing consistently smaller values of A_n compared to herbal crops like basil, and may be less sensitive to different light treatments.

Additional insights are given by Figure 5, which shows the transition from light-limited (RuBP regeneration-limited) photosynthesis rate (A_n) to Rubisco-limited (A_c) photosynthesis rate as a function of irradiance (Figures 5a

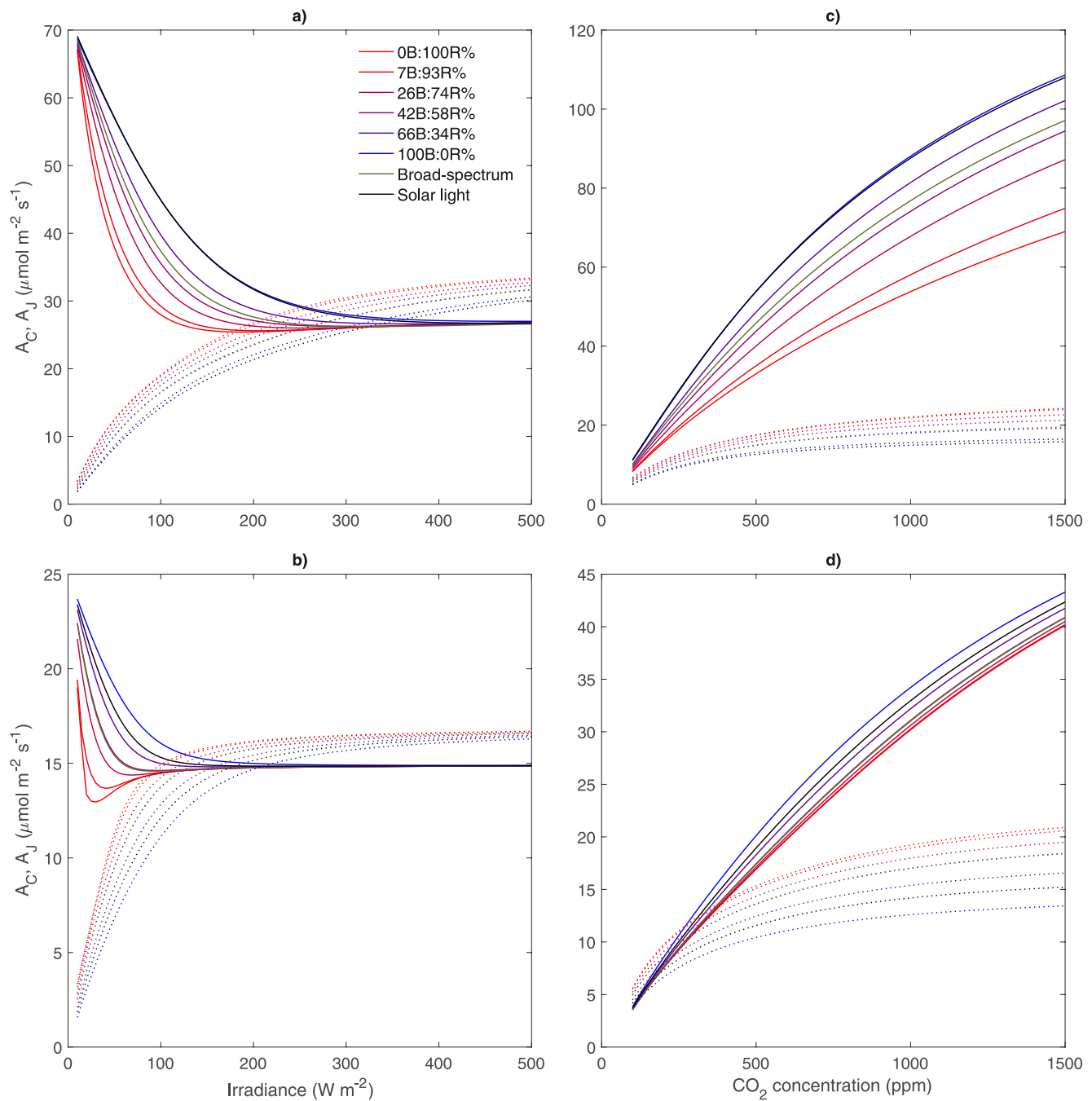


Figure 5. Rubisco-limited (A_C —solid lines) and RuBP-regeneration (i.e., light) limited (A_J —dashed lines) components of photosynthesis rate as a function of (a and b) irradiance and (c and d) air CO_2 concentration, for (a and c) basil and (b and d) strawberry subject to different light treatments. Reference values for the other environmental variables are the same as in Figures 3 and 4.

and 5b) and CO_2 concentration (Figures 5c and 5d), for both crops. For basil, the transition from A_J -limited to A_C -limited photosynthesis occurs later than strawberry (compare Figure 5a with Figure 5b). For both plant types, this transition occurs for red light treatments first and later for solar light and blue light spectra. Interestingly, basil remains always A_J -limited as a function of CO_2 concentration (Figure 5c), at least for the fixed value of irradiance used here (80 W m^{-2}), while strawberry displays a very early transition from A_C to A_J -limited photosynthesis rate (Figure 5d). Overall, this analysis suggests that photo-selective shading may push plants to operate more in RuBP regeneration mode, where the spectrum of light is far more influential.

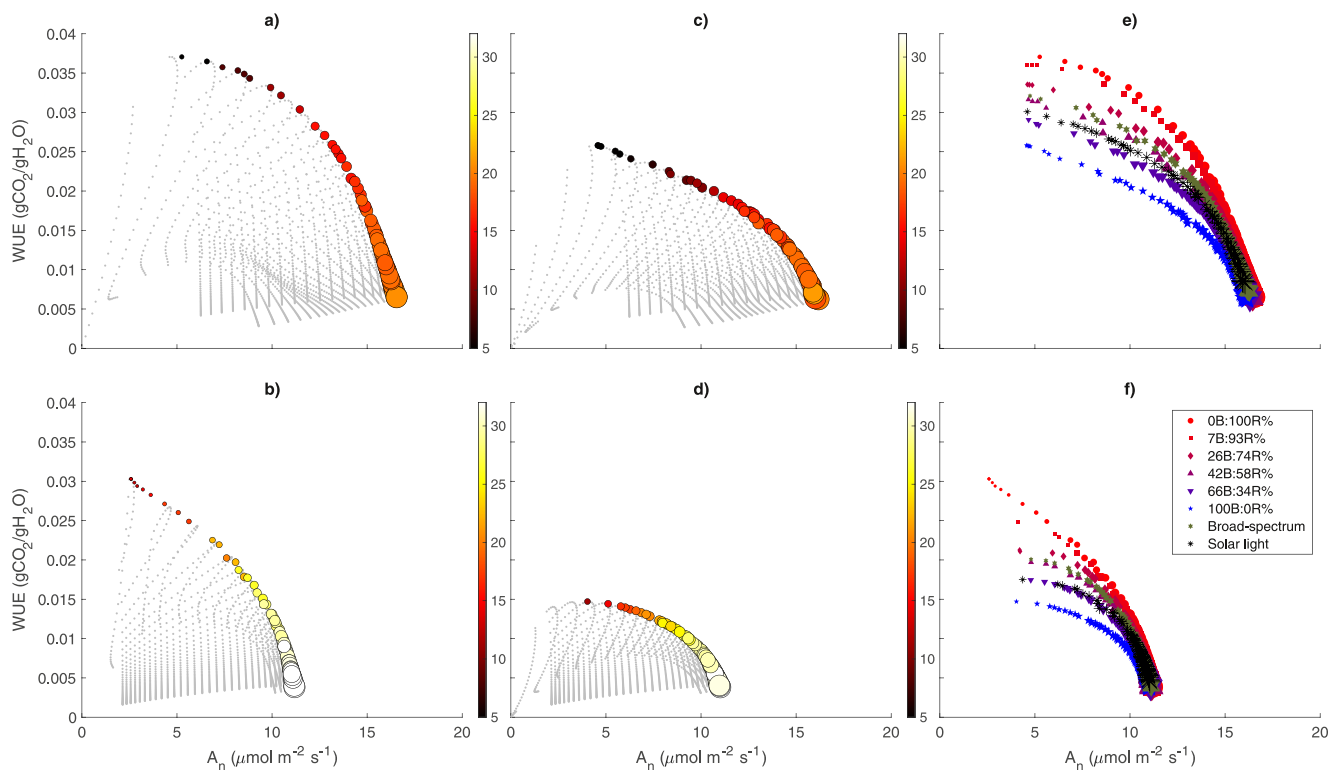


Figure 6. Water use efficiency versus photosynthesis rate for (a, c, and e) basil and (b, d, and f) strawberry subject to (a and b) 100% red light treatment, (c and d) 100% blue light, and (e and f) all light treatments. In panels (a–d), gray dots represent simulation results from the sensitivity analyses, while colored dots represent the Pareto fronts (non-dominated solutions), whereby the size is proportional to irradiance and the color indicates temperature, according with the color bars. Panels (e and f) report the Pareto fronts for each light treatment, with symbol size proportional to irradiance.

From a close inspection of Figures 3 and 4, it is clear that some tradeoffs must exist between photosynthesis rate and WUE, when the two variables are plotted as a function of irradiance and, to a lesser extent, temperature. To quantify these tradeoffs, a multi-objective optimization analysis was carried out aiming at finding the best combinations of environmental factors that result in non-dominated (i.e., Pareto optimal) solutions, that is, points where no variable can improve without worsening the other one. The optimization was performed through the MATLAB® algorithm *paretosearch*, which is able to iteratively compute the Pareto front, based on lower and upper bounds on the input environmental variables. These lower and upper bounds corresponded to the minimum and maximum values of the ranges used in the previous sensitivity analysis. The results of this analysis are reported in Figure 6, with Figures 6a, 6c, and 6e referring to basil and Figures 6b, 6d, and 6f referring to strawberry. The colored dots in the Figure denote the Pareto front (i.e., optimal solutions), with color and size proportional to temperature and irradiance, respectively, while gray dots represent all the simulation results from the sensitivity analysis, plotted in the A_n -WUE space. Figures 6a–6d show that increasing A_n (i.e., crop productivity) is possible only at the expense of WUE, for both plant types and all light treatments (more on this in Figures 6e and 6f). In particular, increasing Pareto-optimal photosynthetic rates are associated with increasing temperatures and irradiance levels (as shown by the color scale and symbol size reflecting irradiance in Figure 6). A wide range of light treatments is demonstrated in Figures 6e and 6f, and confirm that, for both basil and strawberry, the red lighting treatments are more effective than blue lighting, with broad spectrum and solar light in between the two. Also, comparisons between Figures 6a and 6b, as well as between Figures 6c and 6d, highlight that some plant types (strawberry in this case) cannot achieve the same levels of productivity and WUE of other plants (like basil here).

4. Discussion

Solar radiation is perhaps the safest resource that we can bet on its sustainability and reliability, if not even on its possible increase in some regions, as predicted by climate models (Gil et al., 2019). We can see a critical mass of interest and support for land management practices that share the solar light in food and energy co-generation to improve land and water efficiencies and reduce heat stress on plants (Amaducci et al., 2018; Elamri et al., 2018; Feuerbacher et al., 2021). Results of this study can guide this global interest and identify potential applications for those systems. In standard agrivoltaics, crops are grown under fully opaque solar panels, whereby shading can be complete or partial, depending on the arrangement of the PV modules. Recent studies have already demonstrated the socioeconomic potential of such systems (Barron-Gafford et al., 2019; Elamri et al., 2018; Fernández et al., 2022). However, the increasing development of wavelength-selective semi-transparent modules, or “organic PV” (Emmott et al., 2015; Magadley et al., 2022) provide unique opportunities to “harvest” some parts of the incoming light spectrum to generate energy and letting through mostly the parts of the spectrum that are more useful for the plants. To fully reach this potential, accurate plant models are needed that explicitly consider light and PAR spectra to compute the crop productivity. Within this context, the model presented in this work can be a promising first step in this direction.

Results from this work suggest that the blue part of the spectrum is the more promising for energy production, as it carries more potential energy and at the same time it is not the one “preferred” by the plants in terms of photosynthetic activity and WUE. Also, the model predicts that increasing CO₂ concentration enhances the differences between different light treatments, as opposed to increasing irradiance. This, combined with the finding that limiting irradiance may push plants to operate more in light-limited net CO₂ assimilation rate, where the spectrum of light is far more influential, could provide the rationale for boosting the adoption of sunlight management practices, in light of the current growth rate of atmospheric CO₂ concentration, estimated at around 2 ppm/yr (Keenan et al., 2016).

This study also suggests that wavelength-selective agrivoltaic systems may be sensitive to environmental factors and crop type. Spatially, we see better utility of such systems in water-limited areas (as compared to solar radiation-limited), as suggested by Barron-Gafford et al. (2019). From a crop perspective, not all crops are suited for use in agrivoltaics as demonstrated in the comparison between basil and strawberry which showed strawberry is less sensitive to different light treatments. Therefore, this model could be used to preliminarily assess the suitability of different plant species for use in agrivoltaics, provided that the PAR curves, that is, absorbance and quantum yield spectra, are accurate. In this perspective, it should be noted that most plant response spectra (including the ones used here) are based on studies that date back to 50 years ago (Inada, 1976; McCree, 1971), carried out in experimental conditions that might not be representative of the ones typical in agrivoltaic systems. Therefore, more studies are needed to update and re-interpret these important pieces of information, as recently urged by Wu et al. (2019).

Another innovative aspect of this study is related to the stomatal conductance formula used, based on the model proposed by Medlyn et al. (2011) and modified by Kromdijk et al. (2019) to take explicitly into account the light-induced stomatal movements. We highlight here that by using the original model in Medlyn et al. (2011), even with model calibration, we could not reproduce the measured response of stomatal conductance to the different light treatments. This proves that approaches such as the one in Kromdijk et al. (2019) are essential to model the photosynthesis and transpiration rates of plants in response to changing light spectra. We also stress that the stomatal conductance model used here in principle reconciles the empirical approach and the optimal approach, whereby g_s is modeled as an optimization process aimed at maximizing carbon gains while minimizing water losses (Katul et al., 2010). However, it should be noted that Medlyn et al.'s formula for stomatal conductance assumes that photosynthetic rate in the optimization is limited only by RuBP regeneration (Equation 3 in the Methods). This seems to be a reasonable assumption in the case of crops growing under solar panels, where the level of irradiance is expected to be relatively low. Indeed, Figure 4 shows that the range in which photosynthetic rate is limited by the rate of carboxylation (Equation 2 in the Methods) in our simulations is restricted to relatively high values of irradiance. Nevertheless, future studies will be aimed at generalizing the stomatal conductance optimal approach, in order to take into account also the possible limitation of A_n by the rate of carboxylation. This would also give us the opportunity to use a unified model valid for both C3 and C4 plants, also based on optimality theories (Way et al., 2014).

As mentioned above, this study is the first and necessary step toward the development of crop models that can account for the incident light spectral quality, but it is not sufficient. A number of outstanding challenges remain to be addressed to confirm whether our preliminary conclusions can be applied in real world agrivoltaic applications. First, translating gains in photosynthesis to increased crop yield remains uncertain, as increases in photosynthesis alone are likely to be accompanied with increases in autotrophic respiration and other losses (e.g., root exudation). In addition, nitrogen considerations may also be suggestive that higher photosynthetic rates require higher nitrogen (and fertilization), with possible issues for both water and air quality. Second, upscaling from the leaf scale to the entire canopy could lead to different sensitivity outcomes, as canopy-scale processes often do not perfectly reflect leaf-scale findings. Third, the presence of solar panels in agrivoltaic systems is likely to complicate the flow field and may appreciably reduce stomatal conductance (especially if the air is obstructed by solar panels and wind speeds at crop heights are substantially reduced). All these are further challenges for crop models that need to be investigated in future research.

5. Conclusions

We expanded a well-established model of plant photosynthesis and transpiration to explicitly take into account the spectra of incident light and PAR curves (i.e., absorptance and quantum yield). The proposed model satisfactorily reproduces the response of various C3 plant types (lettuce, basil, strawberry) treated with different light spectra in controlled laboratory conditions. A sensitivity analysis to the most important abiotic forcing variables (irradiance, air temperature, humidity, and CO₂ concentration) suggests that the blue part of the light spectrum is the less efficient in terms of carbon assimilation and water use and could be effectively filtered out to produce solar energy. However, the plant response to different light treatments is most likely species-specific; therefore, accurate and updated PAR curves are needed to assess which crops are more suited to be grown in controlled agricultural systems.

In conclusion, we argue that it is time to start thinking about light and solar radiation as resources that can be utilized in optimized food-energy co-generation systems, rather than boundary conditions that we have to deal with in food or energy monocultures. This can foster collaborations between competing groups and bring benefits beyond food and energy, including water conservation, soil health, and ecological restoration. In addition, this effort represents an important first step toward the development of crop models that will be able to simulate crop yield and water use in agrivoltaic systems and other shaded agriculture conditions, with potentially important implications for food and energy co-production and climate change mitigation.

Conflict of Interest

The authors declare no conflicts of interest relevant to this study.

Data Availability Statement

The data and model are available at <https://doi.org/10.5281/zenodo.7331014>.

References

- Abidin, M. A. Z., Mahyuddin, M. N., & Zainuri, M. A. A. M. (2021). Solar photovoltaic architecture and agronomic management in agrivoltaic system: A review. *Sustainability*, *13*(14), 7846. <https://doi.org/10.3390/su13147846>
- Ahmed, H. A., Yu-Xin, T., & Qi-Chang, Y. (2020). Optimal control of environmental conditions affecting lettuce plant growth in a controlled environment with artificial lighting: A review. *South African Journal of Botany*, *130*, 75–89. <https://doi.org/10.1016/j.sajb.2019.12.018>
- Amaducci, S., Yin, X., & Colauzzi, M. (2018). Agrivoltaic systems to optimise land use for electric energy production. *Applied Energy*, *220*, 545–561. <https://doi.org/10.1016/j.apenergy.2018.03.081>
- Amaro de Sales, R., Chaves de Oliveira, E., Buzatto, E., Ferreira de Almeida, R., Alves de Lima, M. J., da Silva Berilli, S., et al. (2021). Photo-selective shading screens as a cover for production of purple lettuce. *Scientific Reports*, *11*(1), 14972. <https://doi.org/10.1038/s41598-021-94437-5>
- Barron-Gafford, G. A., Pavao-Zuckerman, M. A., Minor, R. L., Sutter, L. F., Barnett-Moreno, I., Blackett, D. T., et al. (2019). Agrivoltaics provide mutual benefits across the food–energy–water nexus in drylands. *Nature Sustainability*, *2*(9), 848–855. <https://doi.org/10.1038/s41893-019-0364-5>
- Bastias, R. M., Losciale, P., Chieco, C., & Corelli-Grappadelli, L. (2021). Red and blue netting alters leaf morphological and physiological characteristics in apple trees. *Plants*, *10*(1), 1–16. <https://doi.org/10.3390/plants10010127>
- Buckley, T. N. (2017). Modeling stomatal conductance. *Plant Physiology*, *174*(2), 572–582. <https://doi.org/10.1104/pp.16.01772>

Acknowledgments

MC was supported by a U.S. Department of State J. William Fulbright Research Scholarship. MAN was partly supported by The University of California—Davis, Agricultural Experiment Station, The Multistate Hatch Program W4188 of the USDA, National Institute of Food and Agriculture, and a Ben and Christine Sloss gift to support research on agrivoltaics. Figure 1 was prepared in collaboration with Impact Media Lab. The authors thank two anonymous reviewers, whose comments helped to improve the manuscript.

- Chamas, Z., Abou Najm, M., Al-Hindi, M., Yassine, A., & Khattar, R. (2021). Sustainable resource optimization under water-energy-food-carbon nexus. *Journal of Cleaner Production*, 278, 123894. <https://doi.org/10.1016/j.jclepro.2020.123894>
- Chen, X. L., Li, Y. L., Wang, L. C., & Guo, W. Z. (2021). Red and blue wavelengths affect the morphology, energy use efficiency and nutritional content of lettuce (*Lactuca sativa* L.). *Scientific Reports*, 11(1), 8374. <https://doi.org/10.1038/s41598-021-87911-7>
- Clavijo-Herrera, J., van Santen, E., & Gómez, C. (2018). Growth, water-use efficiency, stomatal conductance, and nitrogen uptake of two lettuce cultivars grown under different percentages of blue and red light. *Horticulturae*, 4(3), 16. <https://doi.org/10.3390/horticulturae4030016>
- Daly, E., Porporato, A., & Rodríguez-Iturbe, I. (2004). Coupled dynamics of photosynthesis, transpiration and soil water balance. Part I: Upscaling from hourly to daily level. *Journal of Hydrometeorology*, 5(3), 546–558. [https://doi.org/10.1175/1525-7541\(2004\)005<0546:cdopta>2.0.co;2](https://doi.org/10.1175/1525-7541(2004)005<0546:cdopta>2.0.co;2)
- Danziger, N., & Bernstein, N. (2021). Light matters: Effect of light spectra on cannabinoid profile and plant development of medical cannabis (*Cannabis sativa* L.). *Industrial Crops and Products*, 164, 113351. <https://doi.org/10.1016/j.indcrop.2021.113351>
- Duan, Q., Sorooshian, S., & Gupta, V. K. (1994). Optimal use of the SCE-UA global optimization method for calibrating watershed models. *Journal of Hydrology*, 158(3–4), 265–284. [https://doi.org/10.1016/0022-1694\(94\)90057-4](https://doi.org/10.1016/0022-1694(94)90057-4)
- Elamri, Y., Cheviron, B., Lopez, J. M., Dejean, C., & Belaud, G. (2018). Water budget and crop modelling for agrivoltaic systems: Application to irrigated lettuces. *Agricultural Water Management*, 208, 440–453. <https://doi.org/10.1016/j.agwat.2018.07.001>
- Emmott, C. J. M., Röhr, J. A., Campoy-Quiles, M., Kirchartz, T., Urbina, A., Ekins-Daukes, N. J., & Nelson, J. (2015). Organic photovoltaic greenhouses: A unique application for semi-transparent PV? *Energy & Environmental Science*, 8(4), 1317–1328. <https://doi.org/10.1039/c4ee03132f>
- Fang, L., Ma, Z., Wang, Q., Nian, H., Ma, Q., Huang, Q., & Mu, Y. (2021). Plant growth and photosynthetic characteristics of soybean seedlings under different LED lighting quality conditions. *Journal of Plant Growth Regulation*, 40(2), 668–678. <https://doi.org/10.1007/s00344-020-10131-2>
- Farquhar, G. D., von Caemmerer, S., & Berry, J. A. (1980). A biochemical model of photosynthetic CO₂ assimilation in leaves of C₃ species. *Planta*, 149(1), 78–90. <https://doi.org/10.1007/BF00386231>
- Fatichi, S., Ivanov, V. Y., & Caporali, E. (2012). A mechanistic ecohydrological model to investigate complex interactions in cold and warm water-controlled environments: 1. Theoretical framework and plot-scale analysis. *Journal of Advances in Modeling Earth Systems*, 4(2), M05002. <https://doi.org/10.1029/2011MS000086>
- Fernández, E. F., Villar-Fernández, A., Montes-Romero, J., Ruiz-Torres, L., Rodrigo, P. M., Manzaneda, A. J., & Almonacid, F. (2022). Global energy assessment of the potential of photovoltaics for greenhouse farming. *Applied Energy*, 309, 118474. <https://doi.org/10.1016/j.apenergy.2021.118474>
- Feuerbacher, A., Laub, M., Högy, P., Lippert, C., Pataczek, L., Schindele, S., et al. (2021). An analytical framework to estimate the economics and adoption potential of dual land-use systems: The case of agrivoltaics. *Agricultural Systems*, 192, 103193. <https://doi.org/10.1016/j.agsy.2021.103193>
- Gil, V., Gaertner, M. A., Gutierrez, C., & Losada, T. (2019). Impact of climate change on solar irradiation and variability over the Iberian Peninsula using regional climate models. *International Journal of Climatology*, 39(3), 1733–1747. <https://doi.org/10.1002/joc.5916>
- Głowacka, K., Kromdijk, J., Kucera, K., Xie, J., Cavanagh, A. P., Leonelli, L., et al. (2018). Photosystem II Subunit S overexpression increases the efficiency of water use in a field-grown crop. *Nature Communications*, 9(1), 868. <https://doi.org/10.1038/s41467-018-03231-x>
- Gueymard, C. A., Myers, D., & Emery, K. (2002). Proposed reference irradiance spectra for solar energy systems testing. *Solar Energy*, 73(6), 443–467. [https://doi.org/10.1016/S0038-092X\(03\)00005-7](https://doi.org/10.1016/S0038-092X(03)00005-7)
- Higgins, C. W., & Najm, M. A. (2020). An organizing principle for the water-energy-food nexus. *Sustainability*, 12(19), 8135. <https://doi.org/10.3390/su12198135>
- Inada, K. (1976). Action spectra for photosynthesis in higher plants. *Plant and Cell Physiology*, 17(2), 355–365. <https://doi.org/10.1093/oxford-journals.pcp.a075288>
- Inada, K., & Nishiyama, F. (1987). Growth responses of sun and shade plants in simulated vegetation shade and neutral shade. *Japanese Journal of Crop Science*, 56(1), 99–108. <https://doi.org/10.1626/jcs.56.99>
- Kang, J. H., Yoon, H. I., Lee, J. M., Kim, J. P., & Son, J. E. (2021). Electron transport and photosynthetic performance in *Fragaria* × *anassa* Duch. acclimated to the solar spectrum modified by a spectrum conversion film. *Photosynthesis Research*, 151(1), 31–46. <https://doi.org/10.1007/s11220-021-00875-7>
- Kattge, J., & Knorr, W. (2007). Temperature acclimation in a biochemical model of photosynthesis: A reanalysis of data from 36 species. *Plant, Cell and Environment*, 30(9), 1176–1190. <https://doi.org/10.1111/j.1365-3040.2007.01690.x>
- Katul, G., Manzoni, S., Palmroth, S., & Oren, R. (2010). A stomatal optimization theory to describe the effects of atmospheric CO₂ on leaf photosynthesis and transpiration. *Annals of Botany*, 105(3), 431–442. <https://doi.org/10.1093/aob/mcp292>
- Keenan, T. F., Prentice, I. C., Canadell, J. G., Williams, C. A., Wang, H., Raupach, M., & Collatz, G. J. (2016). Recent pause in the growth rate of atmospheric CO₂ due to enhanced terrestrial carbon uptake. *Nature Communications*, 7(1), 13428. <https://doi.org/10.1038/ncomms13428>
- Kim, H. H., Goins, G. D., Wheeler, R. M., & Sager, J. C. (2004). Stomatal conductance of lettuce grown under or exposed to different light qualities. *Annals of Botany*, 94(5), 691–697. <https://doi.org/10.1093/aob/mch192>
- Kromdijk, J., Głowacka, K., & Long, S. P. (2019). Predicting light-induced stomatal movements based on the redox state of plastoquinone: Theory and validation. *Photosynthesis Research*, 141(1), 83–97. <https://doi.org/10.1007/s11220-019-00632-x>
- Leuning, R. (1995). A critical appraisal of a combined stomatal-photosynthesis model for C₃ plants. *Plant, Cell and Environment*, 18(4), 339–355. <https://doi.org/10.1111/j.1365-3040.1995.tb00370.x>
- Lim, S., & Kim, J. (2021). Light quality affects water use of sweet basil by changing its stomatal development. *Agronomy*, 11(2), 303. <https://doi.org/10.3390/agronomy11020303>
- Liu, H., Fu, Y., Wang, M., & Liu, H. (2017). Green light enhances growth, photosynthetic pigments and CO₂ assimilation efficiency of lettuce as revealed by “knock out” of the 480–560 nm spectral waveband. *Photosynthetica*, 55(1), 144–152. <https://doi.org/10.1007/s11099-016-0233-7>
- Magadley, E., Kabha, R., Dakka, M., Teitel, M., Friman-Peretz, M., Kacira, M., et al. (2022). Organic photovoltaic modules integrated inside and outside a polytunnel roof. *Renewable Energy*, 182, 163–171. <https://doi.org/10.1016/j.renene.2021.10.012>
- Marigliano, L. E., Yu, R., Torres, N., Tanner, J. D., Battany, M., & Kurtural, S. K. (2022). Photosensitive shade films mitigate heat wave damage by reducing anthocyanin and flavonol degradation in grapevine (*Vitis vinifera* L.) berries. *Frontiers in Agronomy*, 4, 898870. <https://doi.org/10.3389/fagro.2022.898870>
- Martínez-Lüscher, J., Chen, C. C. L., Brillante, L., & Kurtural, S. K. (2017). Partial solar radiation exclusion with color shade nets reduces the degradation of organic acids and flavonoids of grape berry (*Vitis vinifera* L.). *Journal of Agricultural and Food Chemistry*, 65(49), 10693–10702. <https://doi.org/10.1021/acs.jafc.7b04163>
- McCree, K. J. (1971). The action spectrum, absorptance and quantum yield of photosynthesis in crop plants. *Agricultural Meteorology*, 9, 191–216. [https://doi.org/10.1016/0002-1571\(71\)90022-7](https://doi.org/10.1016/0002-1571(71)90022-7)

- Medlyn, B. E., Duursma, R. A., Eamus, D., Ellsworth, D. S., Prentice, I. C., Barton, C. V. M., et al. (2011). Reconciling the optimal and empirical approaches to modelling stomatal conductance. *Global Change Biology*, 17(6), 2134–2144. <https://doi.org/10.1111/j.1365-2486.2010.02375.x>
- Mochizuki, Y., Sekiguchi, S., Horiuchi, N., Aung, T., & Ogiwara, I. (2019). Photosynthetic characteristics of individual strawberry (*Fragaria × ananassa* Duch.) leaves under short-distance lightning with blue, green, and red led lights. *HortScience*, 54(3), 452–458. <https://doi.org/10.21273/HORTSCI13560-18>
- Muneer, S., Kim, E. J., Park, J. S., & Lee, J. H. (2014). Influence of green, red and blue light emitting diodes on multiprotein complex proteins and photosynthetic activity under different light intensities in lettuce leaves (*Lactuca sativa* L.). *International Journal of Molecular Sciences*, 15(3), 4657–4670. <https://doi.org/10.3390/ijms15034657>
- Nguyen, T. K. L., & Oh, M. M. (2021). Physiological and biochemical responses of green and red perilla to LED-based light. *Journal of the Science of Food and Agriculture*, 101(1), 240–252. <https://doi.org/10.1002/jsfa.10636>
- Ogren, E., & Evans, J. R. (1993). Photosynthetic light-response curves. *Planta*, 189(2), 182–190. <https://doi.org/10.1007/BF00195075>
- Pattison, P. M., Tsao, J. Y., Brainard, G. C., & Bugbee, B. (2018). LEDs for photons, physiology and food. *Nature*, 563(7732), 493–500. <https://doi.org/10.1038/s41586-018-0706-x>
- Pennisi, G., Blasioli, S., Cellini, A., Maia, L., Crepaldi, A., Braschi, I., et al. (2019). Unraveling the role of Red: Blue LED lights on resource use efficiency and nutritional properties of indoor grown sweet basil. *Frontiers of Plant Science*, 10, 305. <https://doi.org/10.3389/fpls.2019.00305>
- Pennisi, G., Pistillo, A., Orsini, F., Cellini, A., Spinelli, F., Nicola, S., et al. (2020). Optimal light intensity for sustainable water and energy use in indoor cultivation of lettuce and basil under red and blue LEDs. *Scientia Horticulturae*, 272, 109508. <https://doi.org/10.1016/j.scienta.2020.109508>
- Pennisi, G., Pistillo, A., Orsini, F., Gianquinto, G., Fernandez, J. A., Crepaldi, A., & Nicola, S. (2020). Improved red and blue ratio in LED lighting for indoor cultivation of basil. *Acta Horticulturae*, 1271, 115–118. <https://doi.org/10.17660/ActaHortic.2020.1271.16>
- Pinho, P., Jokinen, K., & Halonen, L. (2012). Horticultural lighting - present and future challenges. *Lighting Research and Technology*, 44(4), 427–437. <https://doi.org/10.1177/1477153511424986>
- Pundir, R. K., Pathak, A., Joshi, N., Bagri, D. S., & Upadhyaya, C. P. (2020). Irradiation studies of LED light spectra on the growth and development of potato (*Solanum tuberosum* L.). *Plant Science Today*, 7(3), 406–416. <https://doi.org/10.14719/PST.2020.7.3.797>
- Ragaveena, S., Shirly Edward, A., & Surendran, U. (2021). Smart controlled environment agriculture methods: A holistic review. *Reviews in Environmental Science and Biotechnology*, 20(4), 887–913. <https://doi.org/10.1007/s11157-021-09591-z>
- Ringler, C., Willenbockel, D., Perez, N., Rosegrant, M., Zhu, T., & Matthews, N. (2016). Global linkages among energy, food and water: An economic assessment. *Journal of Environmental Studies and Sciences*, 6(1), 161–171. <https://doi.org/10.1007/s13412-016-0386-5>
- Samuoliénė, G., Viršilė, A., Haimi, P., & Miliauskienė, J. (2020). Photoresponse to different lighting strategies during red leaf lettuce growth. *Journal of Photochemistry and Photobiology B: Biology*, 202, 111726. <https://doi.org/10.1016/j.jphotobiol.2019.111726>
- Smith, H. L., Mcausland, L., & Murchie, E. H. (2017). Don't ignore the green light: Exploring diverse roles in plant processes. *Journal of Experimental Botany*, 68(9), 2099–2110. <https://doi.org/10.1093/jxb/erx098>
- Waller, R., Kacira, M., Magadley, E., Teitel, M., & Yehia, I. (2021). Semi-transparent organic photovoltaics applied as greenhouse shade for spring and summer tomato production in arid climate. *Agronomy*, 11(6), 1152. <https://doi.org/10.3390/agronomy11061152>
- Way, D. A., Katul, G. G., Manzoni, S., & Vico, G. (2014). Increasing water use efficiency along the C3 to C4 evolutionary pathway: A stomatal optimization perspective. *Journal of Experimental Botany*, 65(13), 3683–3693. <https://doi.org/10.1093/jxb/eru205>
- Wu, B.-S., Rufyikiri, A.-S., Orsat, V., & Lefsrud, M. G. (2019). Re-interpreting the photosynthetically action radiation (PAR) curve in plants. *Plant Science*, 289, 110272. <https://doi.org/10.1016/j.plantsci.2019.110272>

References From the Supporting Information

- Kandel, B. P. (2020). Spad value varies with age and leaf of maize plant and its relationship with grain yield. *BMC Research Notes*, 13(1), 475. <https://doi.org/10.1186/s13104-020-05324-7>
- Kumagai, E., Araki, T., & Kubota, F. (2009). Correlation of chlorophyll meter readings with gas exchange and chlorophyll fluorescence in flag leaves of rice (*Oryza sativa* L.) plants. *Plant Production Science*, 12(1), 50–53. <https://doi.org/10.1626/ppp.12.50>
- Murchie, E. H., & Lawson, T. (2013). Chlorophyll fluorescence analysis: A guide to good practice and understanding some new applications. *Journal of Experimental Botany*, 64(13), 3983–3998. <https://doi.org/10.1093/jxb/ert208>
- Reis, A. R., Favarin, J. L., Malavolta, E., Júnior, J. L., & Moraes, M. F. (2009). Photosynthesis, chlorophylls, and SPAD readings in coffee leaves in relation to nitrogen supply. *Communications in Soil Science and Plant Analysis*, 40(9–10), 1512–1528. <https://doi.org/10.1080/00103620902820373>